

The Chaotic Dripping Faucet: Investigation of Chaotic Behavior in Water Droplet Formation

Joshua Job,¹ Ricky Patel,¹ P. Nicholas Pritchard,¹ and Caleb Royer¹

School of Physics, Georgia Institute of Technology, Atlanta, Georgia 30332, USA

(Dated: 16 December 2011)

The dripping faucet experiment seeks to provide a simple example of a system that exhibits predictable dynamics that transition to an unpredictable, chaotic behavior under certain conditions. The time between water drops falling from a nozzle, is measured with a straightforward experimental setup using a photodiode and a laser. The period, or time between falling drops, is dependent on the flow rate of the water through the nozzle. The photodiode records a drop as the drop breaks the beam of light passing between the diode and laser. The photodiode is interfaced to a computer through an analog to digital converter. The data are analyzed and visualized to characterize the nonlinear dynamics of the system. The dynamics exhibit period-doubling and chaotic behavior. A model is provided for the system, and simulation results are used to interpret the experimentally derived data. The experimental and simulation data are found to follow understood period-doubling and chaotic behavior, however additional modeling and experimentation remains to fully understand the system.

I. INTRODUCTION

The purpose of the chaotic dripping faucet experiment is to characterize the nonlinear dynamics of droplet formation. The chaotic dripping faucet is a canonical, simple example of chaotic behavior, and has been investigated since it was proposed as a model chaotic system by Shaw¹. The expected dynamics include bifurcations and chaos dependent on the input parameters to the sys-

tem, which will be controlled by the experimenters. Through a straightforward experimental setup, the period of falling drops from a nozzle is measured. The period is dependent on the flow rate of fluid through the nozzle. The flow rate can be controlled by changing the flow regulator setting. The dynamics of droplets pinching off and falling from the nozzle are at first predictable, then transition to unpredictable, chaotic behavior as the flow rate of the fluid through the nozzle increases.

It is expected that the dynamics of the falling droplets will show two main regimes: a period doubling regime, and a chaotic regime². Beginning with zero flow rate, as flow rate is increased, the system transitions from a single period to two periods, followed by four periods. If the flow rate is increased farther, the time between drips becomes unpredictable. Plotting the consecutive droplet periods in this region, the chaotic behavior should show a strange attractor. This behavior represents classic chaotic behavior, but it will be shown that the chaotic dripping faucet system does not adhere completely to the understood system dynamics and physical phenomena associated with unimodal maps and the U-sequence³.

The system has been modeled as a damped, harmonic oscillator. The simplest model for the chaotic dripping faucet is that of the mass-spring system given by Shaw¹. This system uses the differential equation of a mass-spring system where the mass increases linearly with time. When the position of the center of mass of the drop reaches a critical value, the mass of the drop is reduced proportionately to the velocity of the drop. This simulates the pinching off of the droplet. Physically, this model is an intuitive description of the system: the water droplet is a mass, and it is driven by the flow of water into it (which increases its mass linearly with

time). The droplet has restoring force due to surface tension and drag force due to viscosity. The equation of motion for this model is:

$$\frac{d(mv)}{dt} = mg - ky - bv$$

where

$$\frac{dm}{dt} = \text{flowrate}$$

$$\frac{dy}{dt} = v$$

g is acceleration due to gravity, y is the droplet height, k is the spring constant from surface tension, b is drag force from viscosity.

An improved version of this model was proposed by Kiyono and Fuchikami². This model is given below, again with g as acceleration due to gravity, z as the height of the droplet center of mass, k as the spring constant from surface tension, γ as the damping from viscosity, a as the nozzle diameter, and v_0 as the velocity of incoming water.

$$m \frac{d^2z}{dt^2} + \left(\frac{dz}{dt} - v_0 \right) \frac{dm}{dt} = mg - kz - \gamma \frac{dz}{dt}$$

$$\frac{dm}{dt} = \text{flowrate} = \pi a^2 v_0$$

where

$$k(m) = \begin{cases} -11.4m + 52.5 & m < 4.61 \\ 0 & m \geq 4.61 \end{cases}.$$

When $z = z_{crit}$, which is the point of droplet breakoff, then $z = z_0$ and $\dot{z} = 0$.

The improved model and the data produced from this model will be used to interpret the experimentally derived data.

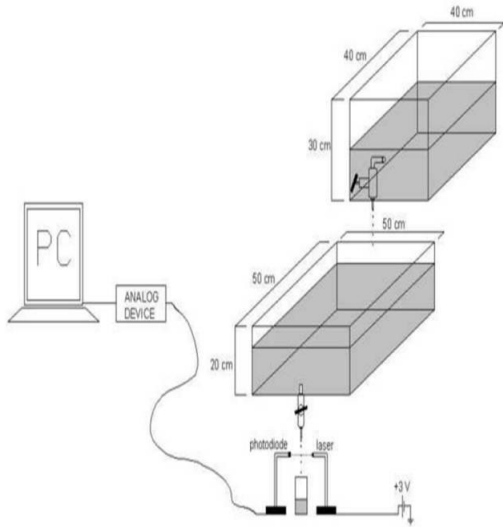


FIG. 1. Proposed experimental setup⁴

II. METHODS

The apparatus is similar in most setups of this experiment⁴, and essentially consists of tanks of fluid flowing through a flow regulator to cause dripping, and a timing mechanism to capture the period of falling drops. For this experiment, the setup was modified from an initial configuration which is depicted in Fig. 1.

A laser was aligned perpendicular to the direction of falling drops, intersecting the path of falling drops. A photodiode was positioned to receive the light from the laser. As the beam was broken by falling drops, the event was captured by the photodiode. A National Instruments USB-6009 Analog to Digital Converter was used to sample the data at 10 kHz and read into a NI LabVIEW Vir-

tual Instrument. This data were then post-processed in MATLAB. In this manner, time history data of the falling drops was acquired and digitized by the computer interface and computer. The resulting time history data were series of pulses, with each pulse being a drop passing through the laser beam, and the period of falling drops measured from these pulses.

In the configuration shown in Fig. 1 the reservoir tank is fed by a feeder tank. The first attempt at a setup did not include a feeder tank, and used a bucket as the reservoir tank. The reservoir tank dripped through small length of rubber tubing as a nozzle, instead of the valve shown in Fig. 1. It was found that the small diameter of the tube being used was causing drops to move laterally as they fell, missing the laser beam. This caused incorrect period measurements, as when a drop is missed the period of the next drop is recorded as double its actual period. It also proved difficult to regulate the flow rate with the bucket setup, as well as measure the flow rate actually coming from the nozzle. For this reason, a second configuration was attempted.

The second attempt used a syringe pump, which was believed to dispense fluid at a well-controlled, specified rate. However, the syringe pump used had undesirable mechanical problems. The syringe pump would visibly

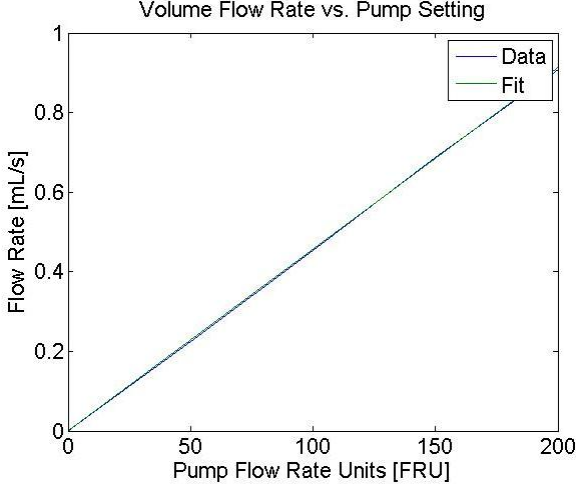


FIG. 2. Pump flow rate regression

oscillate, producing a flow rate that would also oscillate sinusoidally as the product of the mechanical rotation of the pump. Furthermore, the limited volume of the syringe constrained the time that the system could be used to take data.

The final configuration of the experimental setup involved the same laser-photodiode path, but a pump was used to run water through a 5mm diameter flexible tubing. The pump had a built in flow regulator, where flow rate could be set directly. The units of the pump were not listed, so measurements were taken and linearly regressed to provide a conversion from the pump units to SI units. This regression is shown in Fig. 2. The conversion factor was found to be $\frac{mL}{s} = 0.004563FRU$, where FRU are the flow rate units of the pump.

As mentioned previously, the raw data

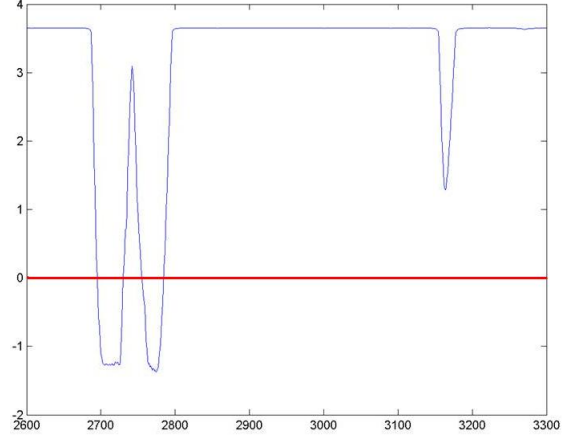


FIG. 3. Raw data with threshold applied

are time histories, with spikes corresponding to points at which the laser beam is broken by a falling drop. A threshold value is chosen, where a spike crossing the threshold constitutes a drop falling through the beam. Online error analysis was necessary since the data captured initially did not seem to match expectations of period doubling or chaotic behavior. It was determined that tiny drops were falling and being emitted from the larger drops, called satellite drops. At first, it was thought that these tiny satellite drops should be counted, and constituted the appearance of period-2 and period-4 droplet formation. It was learned that these satellite drops should be neglected, so the threshold was adjusted in post-processing to eliminate the satellite drops, which appear as shorter peaks in the data. An example of this threshold applied to a raw data point is shown in Fig. 3, where the shorter satellite drop peak

can be seen.

Next, it was found that when a drop crossed the laser beam, both the top and the bottom of the drop were counted as a threshold crossing. This appears as two peaks, or crossings, for a single drop as seen in Fig. 3. The correction for this behavior is known in electrical and computer engineering circles as debouncing, and is done by applying a refractory period. This period is a delay after a crossing has been detected, during which no other crossings are counted. With the error-corrected, post-processed data, Poincaré maps could be generated. These maps are plots of the period of one drop versus the period of the next, which help show when a system is undergoing period doubling and develops patterns in the data.

III. RESULTS

The post-processed data show rich nonlinear dynamics for this system. A period doubling regime begins at approximately 0.319 mL/s, with drops falling at a constant period prior to this point as shown in Fig. 4. As flow rate increases, the drops begin falling with two alternating periods (period-2) as shown in Fig. 5. The pattern for period-2 on the Poincaré map is seen as two clusters corresponding to the two frequencies at which

drips occur¹. The fact that the clusters are symmetric about the line $y=x$ means that the drip frequency alternates between two values. As flow rate increases farther a transition to chaos is seen, where the time between drips is unpredictable. By plotting the data as T_{n+1} vs T_n , or consecutive drop periods on a Poincaré map, the attractors can be seen for the period doubling regime, with strange attractors for the chaotic regime as shown in Fig 6. Any interesting find is that there is a region of period-3 data in the midst of chaotic behavior, as shown in Fig 7. This can be explained as a period window, and from the band plot in Fig. 7b transient chaos can be seen indicating this data is on the border between a periodic window and the neighboring chaotic region.

The model simulation produced data showing single period, period-2, and chaotic behavior. The Poincaré map and band plot for single period simulated data are shown in Fig. 8. Simulated data for period-2 as well as chaotic behavior are shown in Figs. 9 and 10, respectively. It should be mentioned that this model does not fully go chaotic, but rather goes to very high periods which resemble chaos.

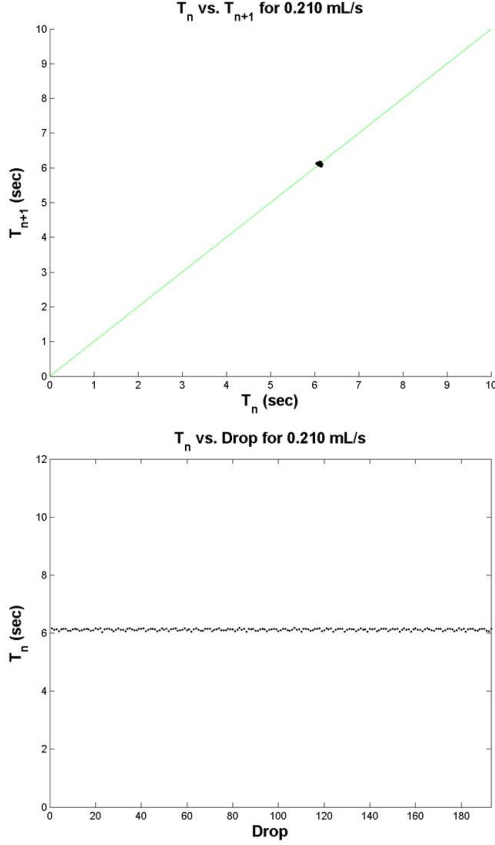


FIG. 4. Post-processed period-1 data. (a) Poincaré map; (b) Period vs. drop number

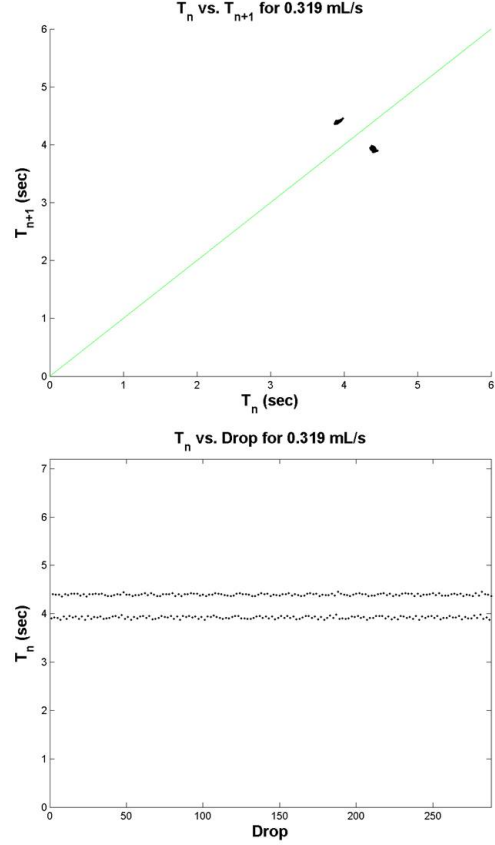


FIG. 5. Post-processed period-2 data. (a) Poincaré map; (b) Period vs. drop number

IV. DISCUSSION

This type of period doubling and chaotic behavior qualitatively matches data in the literature⁵, as well as the data produced by the model discussed in the Introduction².

The bifurcation diagram for the simulation is shown in Fig. 11, and shows distinctly different behavior from what is seen for unimodal maps such as the logistic map. In those cases, following of the U-sequence produces a well-known bifurcation diagram, but here we see repetition in a different form.

We can certainly see period doubling, chaos, all matching between simulation and experimental data and reference data⁵. There is the region of period doubling, where a consistent period bifurcates into two consistent but different periods. This single and period-2 data has been shown in the experimental results, and confirmed by this qualitatively matches reference data⁵. We can also see period-3 data matching the reference data.

Due to the limited resolution of the pump with the current configuration, it was not possible to take data with fine enough flow

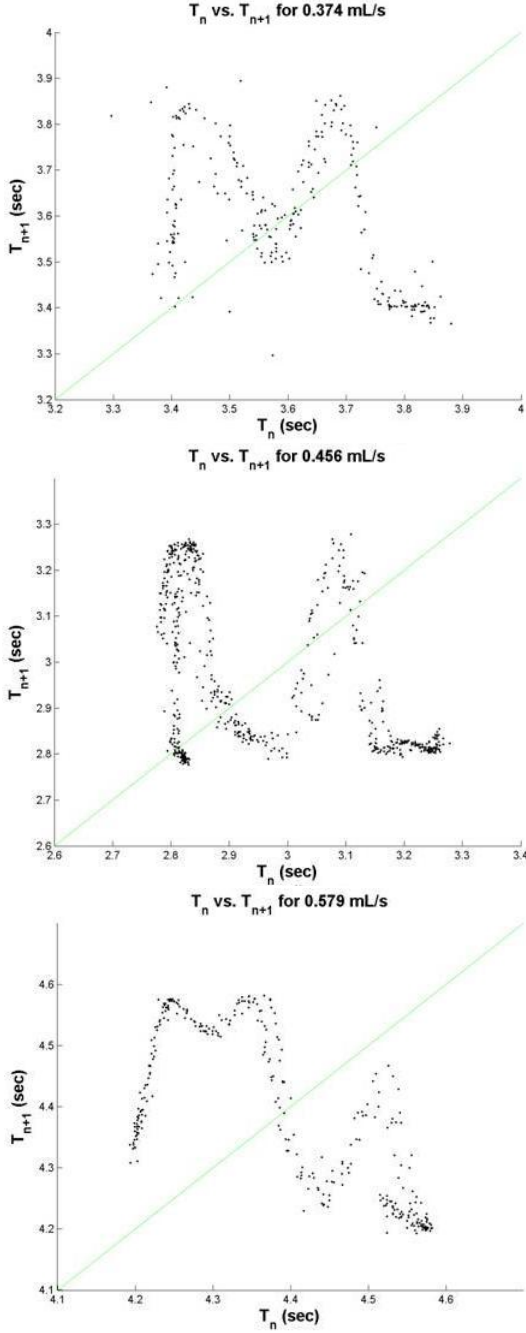


FIG. 6. Poincaré maps for chaotic-regime data. (a) Strange attractor at 0.374 mL/s flow rate; (b) Strange attractor at 0.456 mL/s flow rate; (c) Strange attractor at 0.579 mL/s flow rate;

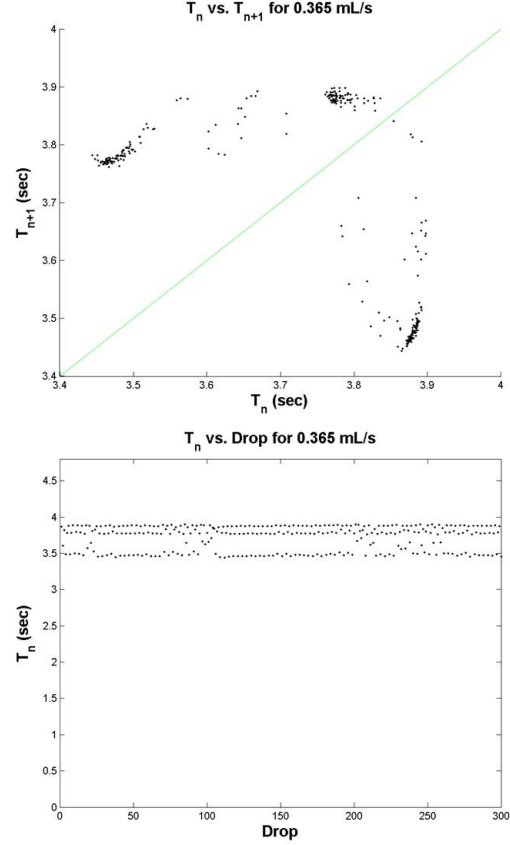


FIG. 7. Post-processed period-3 data. (a) Poincaré map; (b) Period vs. drop number

regulation to reconstruct a bifurcation diagram experimentally. However, given the type of bifurcation data produced from the simulation, it is suspected that the map is in fact not unimodal, and does not follow the U-sequence exactly^{1,3}. Though trends are known for this system, research remains to characterize the actual bifurcation parameters of the chaotic dripping faucet.

In addition to limited flow regulator resolution, it is suspected that pump vibrations and mode interactions contributed to the difficulty reproducing period-4 data. The me-

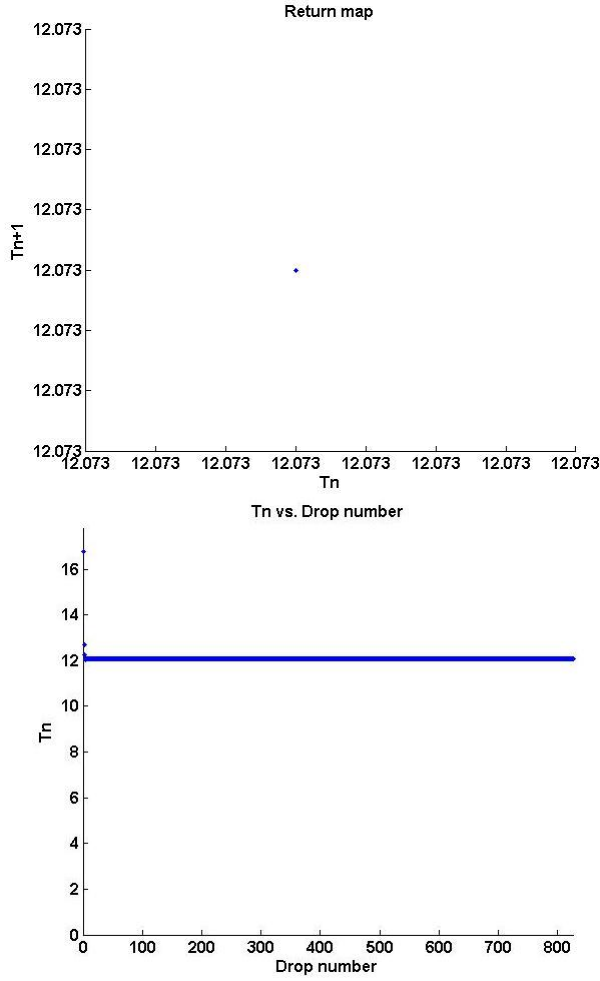


FIG. 8. Simulated period-1 data. (a) Poincaré map; (b) Period vs. drop number

chanical oscillations of the syringe pump were visible to the naked eye, but not with the final setup of pump and flow regulator. Still, patterns on a very small scale formed before period doubling with the pump, indicating some external disturbance. It is suspected that this external disturbance is induced by oscillations in the flow, due to mechanics of the flow regulator. A sinusoidal disturbance such as this could be the reason that finer re-

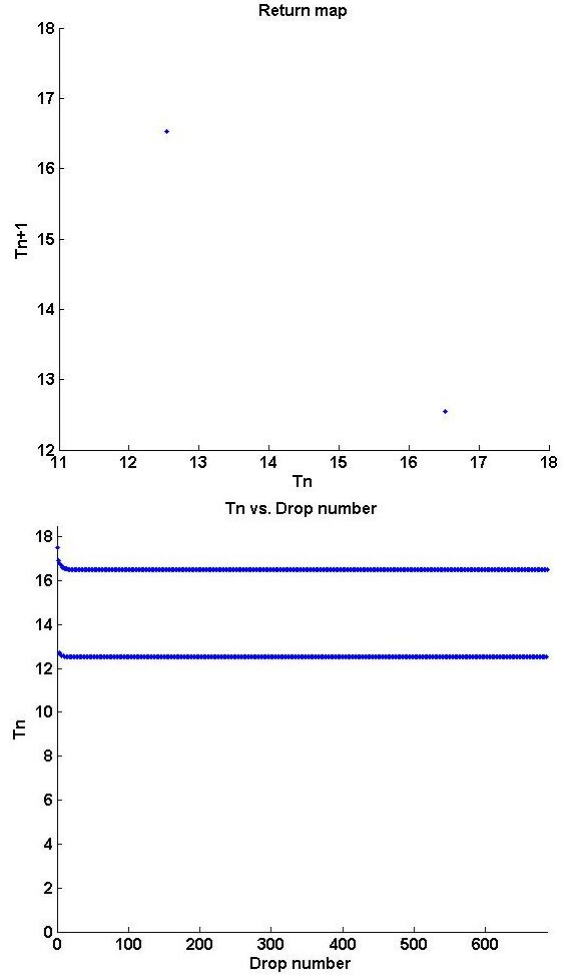


FIG. 9. Simulated period-2 data. (a) Poincaré map; (b) Period vs. drop number

gions of the bifurcation diagram could not be investigated. That is, if there is a sinusoidal disturbance on the input variable, it could cause fluctuation over the period-2/period-4/chaotic region if these regions are sufficiently narrow.

V. CONCLUSION

The data are found to follow understood period-doubling and chaotic behavior. How-

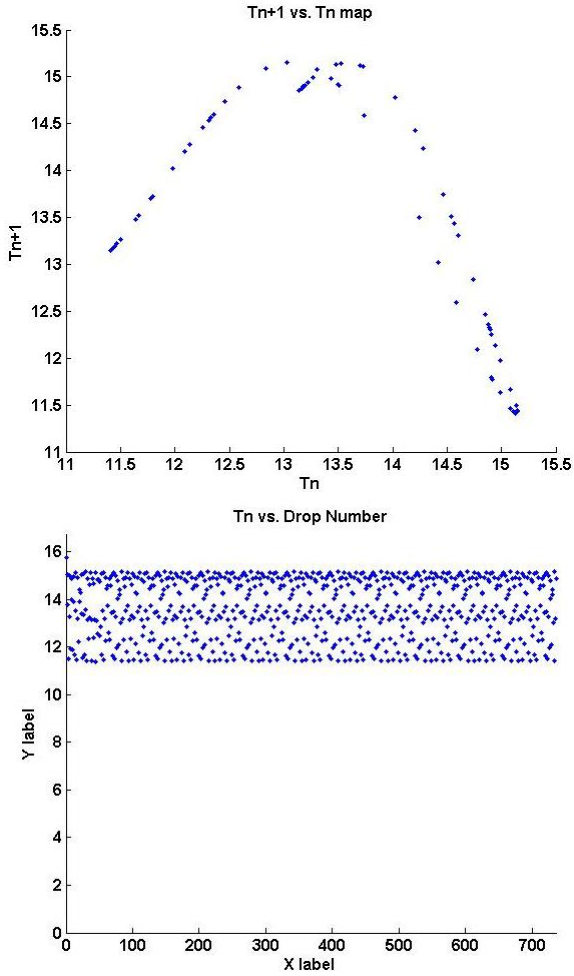


FIG. 10. Simulated Poincaré Map for chaotic data

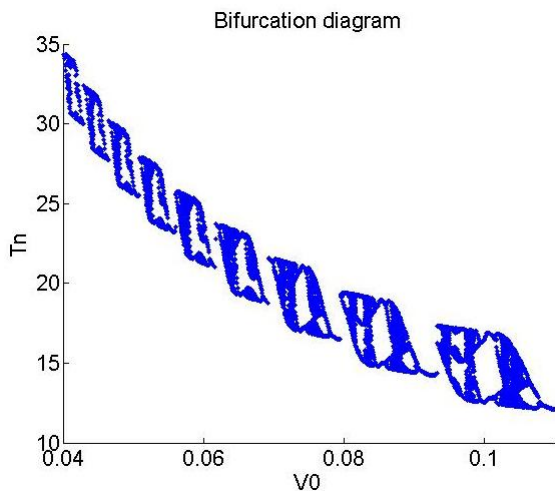


FIG. 11. Simulated bifurcation diagram

ever, additional modeling and experimental work remains to fully understand the system. Recent research has proposed modified models of the system, which seem to predict data well^{2,6}. However, given the limited flow regulator resolution used in this experiment, it is not definitive that these models describe the dynamics of the system, as a unimodal map with a U-sequence of bifurcations could also have produced the data shown above. In short, the bifurcations of this system still not completely understood, nor are the dynamical models completely resolved.

The lessons learned through this research should include fine attention to detail regarding the experimental setup. It is imperative to have accurate flow control and uniform flow rate. It is suggested that shunting the flow to allow finer resolution of the water passing through the nozzle, while still using the crude units of the pump, be performed in order to increase the flow rate resolution. This would allow finer investigation of the 70-90 flow-rate unit (FRU) region of the pump, where the period doubling and chaotic behavior seemed to be most apparent. Furthermore, large nozzle size is important to minimize imperfections and allow harmonic oscillator dynamics. For data collection, care must be taken to exclude satellite drops and debounce the laser-photodiode to remove the double crossings generated by falling drops.

What has been shown is that two routes to chaos appear to be confirmed, as predicted by Dreyer and Hickey. This is seen through the experimental and simulated data showing period doubling, as well as the periodic windows and transient chaos. This qualitative match between data suggest that further research be conducted to produce quantitative, and finer resolution comparisons. Overall, the model and secondary data match the literature and simulation qualitatively.

REFERENCES

¹P. Martien, S. Pope, P. Scott, and R. Shaw, “The chaotic behavior of the leaky faucet,” *Physics Letters A* **110**, 399–404 (1985).

²K. Kiyono, T. Katsuyama, T. Masunaga, and N. Fuchikami, “Picture of the low-dimensional structure in chaotic dripping faucets,” *Journal of the Physical Society of Japan* **68**, 3259–3270 (1999).

³S. H. Strogatz, *Nonlinear Dynamics and Chaos* (Perseus, 1994).

⁴C. E. Somarakis, G. E. Cambourakis, and G. P. Papavassilopoulos, “A new dripping faucet experiment,” *Nonlinear Phenomena in Complex Systems* **11**, 198–204 (2011).

⁵K. Dreyer and F. R. Hickey, “The route to chaos in a dripping water faucet,” *Am. J. Phys* **59**, 619–627 (1991).

⁶P. Coulet, L. Mahadeva, and C. S. Riera, “Hydrodynamical models for the chaotic dripping faucet,” .